

CooPre: Cooperative Pretraining for V2X Cooperative Perception

Seth Z. Zhao¹, Hao Xiang¹, Chenfeng Xu², Xin Xia¹, Bolei Zhou¹, Jiaqi Ma^{1†}

Abstract—Existing Vehicle-to-Everything (V2X) cooperative perception methods rely on accurate multi-agent 3D annotations. Nevertheless, it is time-consuming and expensive to collect and annotate real-world data, especially for V2X systems. In this paper, we present a self-supervised learning method for V2X cooperative perception, which utilizes the vast amount of unlabeled 3D V2X data to enhance the perception performance. Beyond simply extending the previous pre-training methods for point-cloud representation learning, we introduce a novel self-supervised Cooperative Pretraining framework (termed as *CooPre*) customized for a collaborative scenario. We point out that cooperative point-cloud sensing compensates for information loss among agents. This motivates us to design a novel proxy task for the 3D encoder to reconstruct LiDAR point clouds across different agents. Besides, we develop a V2X bird-eye-view (BEV) guided masking strategy which effectively allows the model to pay attention to 3D features across heterogeneous V2X agents (i.e., vehicles and infrastructure) in the BEV space. Noticeably, such a masking strategy effectively pretrains the 3D encoder and is compatible with mainstream cooperative perception backbones. Our approach, validated through extensive experiments on representative datasets (i.e., V2X-Real, V2V4Real, and OPV2V), leads to a performance boost across all V2X settings. Additionally, we demonstrate the framework’s improvements in cross-domain transferability, data efficiency, and robustness under challenging scenarios. The code will be made publicly available.

I. INTRODUCTION

Achieving autonomy in complex and open traffic environments poses significant challenges for single-vehicle vision systems. These systems often suffer from occlusions and a limited perception range due to each vehicle’s singular viewpoint, limiting the capacity of current deep learning approaches to develop a holistic 3D representation in the interacting environment. Vehicle-to-Everything (V2X) Cooperative Perception [1]–[4] emerges as a promising solution by providing each ego agent with a comprehensive understanding of the surrounding environment. Through collaboration among connected agents (vehicles or infrastructure), V2X facilitates the sharing of critical sensing information, thereby extending the perception range and mitigating occlusions. However, this paradigm introduces additional geometrical and topological information that the model must handle, necessitating the exploration of a robust representation that accounts for these elements. Obtaining such a representation often requires a large amount of annotated data, but the scale of current real-world V2X datasets [1], [4]–[8] is still limited

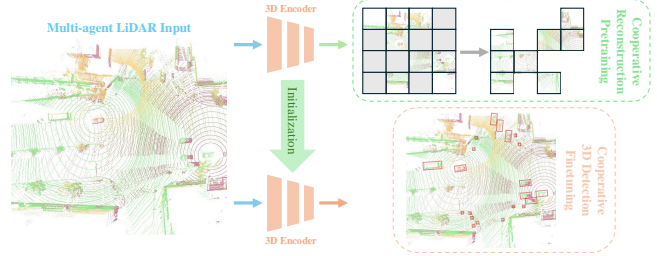


Fig. 1. Illustration of our CooPre framework. Given multi-agent LiDAR input, CooPre pretrains the 3D encoder via a LiDAR point cloud reconstruction task. During the finetuning stage, the initialized 3D encoder will be used for 3D detection task.

compared to single-vehicle counterparts [9]–[12]. Therefore, investigating the representation learning problem within the constraints of current V2X dataset scales is crucial.

In multi-agent perception systems, each ego agent must learn a representation that manages complex agent interaction information to achieve effective cooperation. Specifically, in V2X scenarios, the ego agent must handle different sensor configurations among various agents, which operate at different ranges and placement positions. Capturing this underlying distribution is challenging solely through the supervision of hand-labeled 3D bounding boxes. This complexity poses a challenge for the “train-from-scratch” paradigm, as its learned representation heavily depends on the random initialization of model parameters and the quality and quantity of annotated 3D bounding boxes, thereby affecting overall performance. For example, as discussed in [8], [13]–[16], such approach could be easily perturbed by synchronization or localization errors in real-world scenarios. DiscoNet [17] offers an alternative paradigm by employing a teacher model to guide the student model during training. However, a significant amount of annotations is still required to train an effective teacher model that can facilitate the learning of the student model.

In this paper, based on the aforementioned observations, we propose a simple yet effective self-supervised multi-agent pretraining framework named **CooPre**, showing that *Cooperative Pretraining* enables the model to learn meaningful *prior representation* of the holistic 3D environment before the perception task, as illustrated in Fig.1. Our framework leverages the benefits of unlabeled LiDAR point cloud data transmitted from different agents, allowing the model to reconstruct the point cloud location and learn essential prior knowledge of scenarios (e.g., intersections or corridors) and LiDAR sensor distributions (e.g., range, placement position, and sparsity) of each agent from a bird-eye-view (BEV) per-

[†] Corresponding Author. jiaqima@ucla.edu.

¹ Seth Z. Zhao, Hao Xiang, Xin Xia, Bolei Zhou, and Jiaqi Ma are affiliated with the University of California, Los Angeles. sethzhao506@g.ucla.edu.

² Chenfeng Xu is affiliated with the University of California, Berkeley.

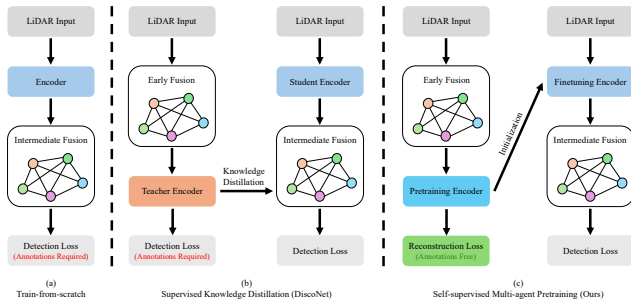


Fig. 2. **Illustration of different training paradigms.** Compared with previous training paradigms, our paradigm uses multi-agent collaboration while being annotation-free.

spective. This design is compatible with current cooperative perception backbones. It makes the reconstruction task more challenging due to the enlarged perception field, which helps mitigate issues related to sparse feature points in far-range and occlusion scenarios. Compared to the other two training paradigms in Fig. 2, our pretraining framework is annotation-free, which is the main contribution to representation learning in V2X cooperative perception.

Following the introduction of this straightforward approach, the remainder of the contribution of this paper focuses on explaining how, where, and why this approach works in V2X cooperative perception scenarios. Our analysis demonstrates: 1) *why pretraining* by showcasing our framework’s strong generalizability to unseen distributions, which is beneficial for domain adaptation, especially when the target dataset is limited in scale; 2) *why reconstruction pretraining* by highlighting our framework’s attention to the geometrical and topological features of rigid-body objects (e.g., cars and trucks); 3) *why multi-agent pretraining* by illustrating improvements in far-range perception and occlusion handling compared to train-from-scratch and single-agent pretraining frameworks [18]–[20]. Through extensive ablation studies and experiments on V2X-Real [1], V2V4Real [8], and OPV2V [21] datasets, we demonstrate the effectiveness of CooPre and shed light on how it works.

II. RELATED WORK

A. Cooperative Perception

Single-vehicle systems struggle with occlusions and long-distance perception in complex traffic environments due to the limitation of the perception range of LiDAR devices. Cooperative systems, on the other hand, enhance detection performance by sharing raw data (Early Fusion), detection outputs (Late Fusion), or intermediate bird-eye-view (BEV) representations (Intermediate Fusion) among connected agents [21]–[23]. With the recent advancement of a variety of simulation and real-world dataset curations [1], [3]–[5], [8], [21], [24], many literature [2], [21]–[23], [25]–[27] have been discussing the algorithmic designs of collaborative modes from vehicle-to-vehicle (V2V) collaboration to vehicle-to-everything (V2X) collaboration in different traffic scenarios. Noticeably, the intermediate fusion strategy has

been the primary direction since it achieves the best trade-off between accuracy and bandwidth requirements. After applying a 3D encoder [28]–[30] to the input LiDAR feature, the intermediate fusion strategy involves projecting 3D features to BEV features where agents will perform interactions before final detection results. For example, AttFuse [21] utilizes a simple agent-wise single-head attention to fuse all features, whereas V2X-ViT [2] presents a unified vision transformer for robust multi-agent multi-scale perception. Despite their targeted designs, these methods all follow “train-from-scratch” paradigm and thus exhibit unstable performance when faced with V2X collaboration challenges, particularly due to sensor data heterogeneity issues [31], [32]. In this paper, we propose a generalizable pretraining framework to enhance the 3D encoders of these backbones. Our framework provides a more robust and versatile representation in the BEV space, directly facilitating the 3D detection task in cooperative perception scenarios from a BEV perspective.

B. Lidar-based Self-supervised Learning

Representation learning in autonomous driving scenarios [18], [20], [33]–[39] has been prevalently investigated in single-vehicle systems. Stemming from the recent advancement of image reconstruction pretraining methods [40], [41], point cloud pretraining reconstruction methods [18]–[20], [37], [42]–[47] are also proven effective in improving backbone model’s robustness and generalizability. Recently, this approach has been applied to 3D representation learning of outdoor point clouds. Occupancy-MAE [37] applies a voxel-wise masking strategy to reconstruct masked voxels and predict occupancy. GD-MAE [19] proposes a multi-level transformer architecture and a multi-scale masking strategy with a lightweight generative decoder to recover masked patches. GeoMAE [20] formulates the pretraining target to be geometric feature predictions, such as pyramid centroid, occupancy, surface normal, and curvature of point clouds. BEV-MAE [18] uses a BEV-guided masking strategy to learn BEV feature representations. Notably, while such pretraining methods have shown great potential in developing general feature representations, their improvement is limited due to the restricted perception field caused by perception range and occlusion in single-vehicle systems. Additionally, there is limited discussion on pretraining in multi-agent systems, with the most similar work being CORE [48], which proposes a BEV map reconstruction as an auxiliary task alongside the original perception target. Our work proposes a multi-agent point cloud reconstruction pretraining framework that synergizes effective cooperative pretraining among vehicle and infrastructure agents in V2X cooperative scenarios.

III. METHOD

A. Overview

The CooPre pretraining pipeline, as shown in Fig.3, involves an early fusion stage where the cooperative agents will transmit their corresponding LiDAR point clouds and metadata to the ego agent. Then we project the vast amount

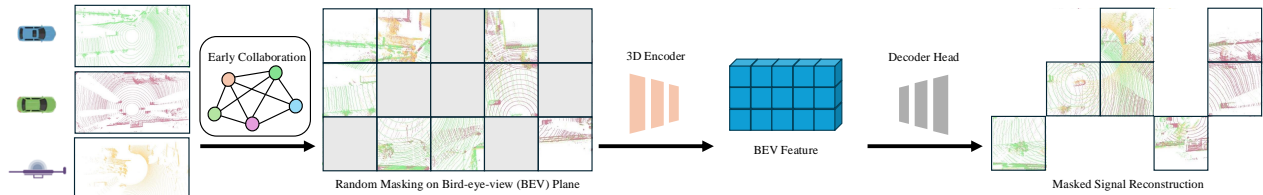


Fig. 3. **Detailed pipeline of our proposed CooPre framework.** During the pretraining stage, the 3D encoder would be asked to perform a cooperative reconstruction task utilizing the vast amount of unlabeled LiDAR point cloud data transmitted from different agents. The masking strategy will be applied in a BEV-guided manner to take into account the reconstruction of far-range point clouds.

of unlabeled LiDAR point cloud data into a bird-eye-view (BEV) plane, where we perform random masking on the point clouds in predefined BEV grids at a fixed ratio. After that, the unmasked point clouds will be passed to the 3D encoder to obtain a BEV feature, which will be passed to a light decoder to reconstruct masked point clouds from both ego and cooperative agents. At the finetuning stage, the 3D encoder would be taken to perform the downstream cooperative perception task along with the designated fusion network [21].

B. V2X BEV-guided Masking Strategy

Intuition. In a BEV perspective, directly applying a random masking strategy will often lead to the fact of masking out most of the ego agent’s near-range point cloud without much attention to the far-range point cloud. This makes the pretraining task hard to learn the representation in far ranges. A BEV-guided masking strategy will mitigate this problem by masking the predefined BEV grid that evenly divides the BEV space. However, from a single-agent perspective, such a masking strategy often results in a large number of BEV grids with a sparse point cloud inside each grid, making the self-supervision hard and inaccurate. Multi-agent collaboration becomes powerful as it provides more point cloud occupation from other collaborative agents in that BEV grid with sparse point clouds. Therefore, we extend the BEV-guided masking strategy [18] to a V2X collaborative scenario.

V2X LiDAR Point Clouds and Metadata Sharing. In the V2X cooperative scenario, suppose we have ego agent A_{ego} and a set of N cooperative agents A_i for $i \in \{1 \dots N\}$ within the communication range, where each agent could be either Connected Autonomous Vehicle (CAV) or infrastructure. During the pretraining stage, each cooperative agent A_i shares LiDAR point clouds and metadata information, such as poses, extrinsics, and agent type, to A_{ego} . We assume the transmission of LiDAR point clouds and metadata is well-synchronized. Consequently, after projecting the point clouds of each cooperative agent to the ego agent’s coordinate, the perception point cloud field of the ego agent A_{ego} includes its own LiDAR point clouds P_{ego} as well as the LiDAR point clouds P_i from each cooperative agent A_i . We refer to the collection of projected LiDAR point clouds from cooperative agents as $P_{coop} = \bigcup_i P_i$.

Masking Strategy. For each ego agent A_{ego} , given the perception range and the resolution, we construct a BEV

space of $X \times Y \times C$ with a set of BEV grids $g_{i,j}$ with a predefined voxel size. After that, for each LiDAR point $p_k \in P_{ego} \cup P_{coop}$, we project it onto a corresponding BEV grid $g_{i,j}$ based on its x, y coordinates. With the help of projected point clouds from cooperative agents, the number of empty BEV grids largely decreases. We then randomly apply a high masking ratio towards non-empty BEV grids, where the point clouds inside the grid will be masked and replaced by learnable point cloud tokens. These tokens will be used alongside with visible point clouds to perform reconstruction target with a light-weight decoder.

C. Reconstruction Objective

As the number of point clouds varies in each masked BEV grid, we designate the lightweight decoder to output a fixed number of point clouds for reconstruction and utilize the Chamfer distance loss as the learning objective. Specifically, suppose in the masked BEV grid $g_{i,j}$, the reconstruction loss is defined as the following equation between predicted point clouds \hat{P} and groundtruth point clouds P :

$$L_{rec}(\hat{P}, P) = \frac{1}{|\hat{P}|} \sum_{\hat{p}_i \in \hat{P}} \min_{p_j \in P} \|p_i - \hat{p}_j\|_2 + \frac{1}{|P|} \sum_{p_i \in P} \min_{\hat{p}_j \in \hat{P}} \|p_i - \hat{p}_j\|_2 \quad (1)$$

Note that the groundtruth point clouds in each masked grid contain a mixture of points from P_{ego} and P_{coop} .

IV. EXPERIMENTS

A. Experiment Setting

Datasets. We evaluate our method on three datasets, namely V2X-Real [1], V2V4Real [8], and OPV2V [21]. V2X-Real is a large-scale, real-world V2X dataset that encompasses all V2X collaboration modes, including vehicle-centric (VC), infrastructure-centric (IC), vehicle-to-vehicle (V2V), and infra-to-infra (I2I). LiDAR sensors for this dataset were embodied with different sensor configurations and deployed in both intersection and corridor scenarios. Note that except for the V2V subset in the V2X-Real dataset, the rest of the subsets all exhibit such LiDAR sensor heterogeneity property. We also examine the effectiveness of our pretraining method on V2V4Real and OPV2V, two well-established benchmarks for real-world and simulated V2V cooperative perception.

Evaluation Metrics. Following previous evaluation protocols [1], [8], [21], we adopt the Average Precisions (AP) at the specified Intersection-over-Union (IoU) threshold as

TABLE I
PERFORMANCE ON V2X-REAL DATASET. GREEN DENOTES THE IMPROVEMENTS OVER THE BASELINE ATTfuse BACKBONE.

Dataset	Method	Car		Pedestrian		Truck		Mean	
		AP0.3	AP0.5	AP0.3	AP0.5	AP0.3	AP0.5	AP0.3	AP0.5
V2X-Real VC	No Fusion	51.0	48.0	35.8	20.4	38.9	36.3	41.9	34.9
	Early Fusion	60.2	58.2	36.2	21.0	45.3	43.3	47.2	40.8
	Late Fusion	59.0	56.5	36.7	17.6	44.0	39.7	46.5	37.9
	AttFuse [21]	67.7	65.8	45.0	27.6	55.5	52.0	56.1	48.5
	CooPre	71.5 ^{+3.8}	70.2 ^{+4.4}	46.9 ^{+1.9}	28.0 ^{+0.4}	61.9 ^{+6.4}	58.3 ^{+6.3}	60.1 ^{+4.0}	52.2 ^{+3.7}
V2X-Real V2V	No Fusion	49.8	47.7	43.6	28.7	38.3	37.0	43.9	37.8
	Early Fusion	62.5	60.0	43.3	28.1	47.3	44.7	51.0	44.3
	Late Fusion	51.6	50.0	44.6	29.1	37.1	35.8	44.4	38.3
	AttFuse [21]	66.9	65.3	46.0	30.4	53.8	50.2	55.5	48.6
	CooPre	71.4 ^{+4.5}	70.1 ^{+4.8}	49.7 ^{+3.7}	33.7 ^{+3.3}	57.5 ^{+3.7}	55.5 ^{+5.3}	59.5 ^{+4.0}	53.1 ^{+4.5}
V2X-Real IC	No Fusion	55.7	48.6	35.2	20.4	46.3	45.5	45.8	38.2
	Early Fusion	73.6	66.2	45.0	25.7	49.9	47.4	56.2	46.4
	Late Fusion	74.5	72.5	47.8	27.4	66.1	57.8	62.8	52.6
	AttFuse [21]	84.5	82.1	61.0	40.6	59.9	59.1	68.5	60.6
	CooPre	86.2 ^{+1.7}	84.1 ^{+2.0}	60.5 ^{-0.5}	39.3 ^{-1.3}	61.5 ^{+1.6}	61.0 ^{+1.9}	69.4 ^{+0.9}	61.4 ^{+0.8}
V2X-Real I2I	No Fusion	67.3	61.5	49.2	32.3	53.2	49.0	56.6	47.6
	Early Fusion	69.3	63.4	51.9	32.5	55.5	52.1	58.9	49.4
	Late Fusion	79.6	78.0	67.3	46.7	64.4	55.8	70.4	60.2
	AttFuse [21]	83.4	81.9	67.0	44.8	63.6	62.8	71.3	63.2
	CooPre	84.6 ^{+1.2}	82.7 ^{+0.8}	66.5 ^{-0.5}	45.2 ^{+0.4}	65.2 ^{+1.6}	62.5 ^{-0.3}	72.1 ^{+0.8}	63.5 ^{+0.3}

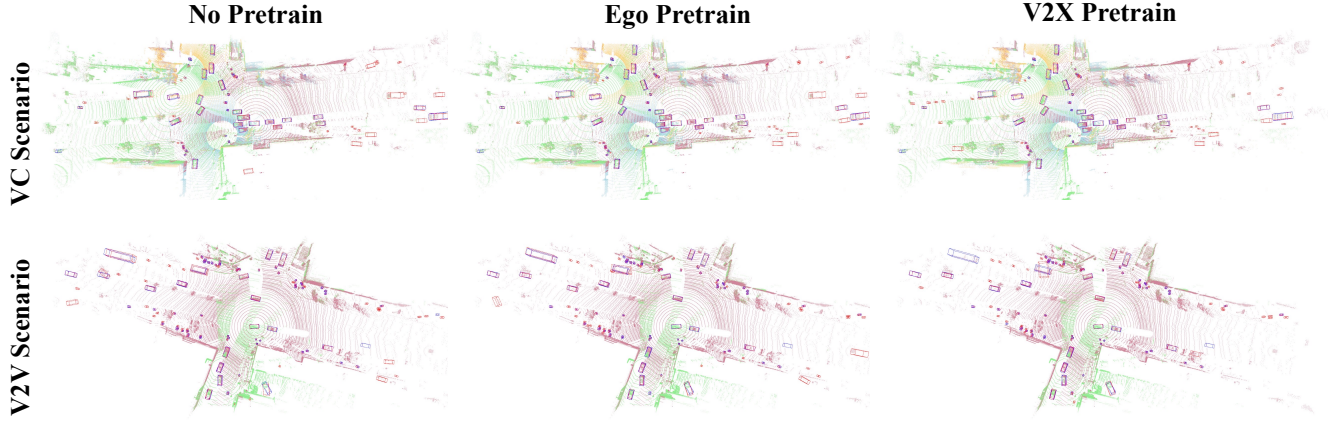


Fig. 4. Comparison of perception performance with different training paradigms in V2X-Real VC and V2V datasets. In comparison to train-from-scratch and single-agent pretraining methods, our multi-agent pretraining yields more robust perception capabilities in scenarios involving occlusions and long-range perception. Particularly, the occurrence of false perceptions significantly decreases in far-range scenarios where point cloud features are sparse. Blue and red 3D bounding boxes correspond to the ground-truth and detection outputs, respectively.

TABLE II
PERFORMANCE ON V2V4REAL DATASET. GREEN DENOTES THE IMPROVEMENTS OVER THE BASELINE ATTfuse BACKBONE.

Method	Overall	Sync (AP0.5/0.7)			Overall	Async (AP0.5/0.7)		
		0-30m	30m-50m	50m-100m		0-30m	30m-50m	50m-100m
No Fusion	52.6/36.2	76.6/58.7	45.9/28.7	10.0/5.0	52.6/36.2	76.6/58.7	45.9/28.7	10.0/5.0
Early Fusion	66.7/34.5	83.3/48.9	51.0/25.3	48.4/19.9	59.5/28.7	82.5/46.2	43.5/21.1	29.8/9.0
Late Fusion	69.9/40.2	81.4/44.0	60.7/38.5	56.9/36.2	63.9/32.5	78.9/40.3	56.8/32.9	39.4/16.8
AttFuse [21]	71.2/44.2	87.3/55.5	55.6/39.8	51.1/25.7	63.8/34.9	85.7/51.4	47.8/31.0	33.4/10.5
CooPre	74.3/49.3 ^{+3.1/5.1}	87.4/60.2 ^{+0.1/4.7}	63.4/45.2 ^{+7.8/5.4}	55.6/32.0 ^{+4.5/6.3}	66.1/39.9 ^{+2.3/5.0}	85.9/57.0 ^{+0.2/5.6}	54.3/34.9 ^{+6.5/3.9}	36.1/14.0 ^{+2.7/3.5}

the metric to evaluate the detection performance. For V2X-Real [1] dataset, we evaluate the performance of different subclasses (i.e. vehicle, pedestrian, and truck) and a final

mean average precision (mAP) at the threshold of 0.3 and 0.5. For V2V4Real [8] dataset, we evaluate the performance of the vehicle class at the threshold of 0.5 and 0.7 in both

TABLE III

PERFORMANCE ON OPV2V DATASET. GREEN DENOTES THE IMPROVEMENTS OVER THE BASELINE ATTfuse BACKBONE.

Method	Default		Culver	
	AP0.5	AP0.7	AP0.5	AP0.7
No Fusion	71.3	60.4	64.6	51.7
Early Fusion	87.7	81.3	82.1	73.8
Late Fusion	84.6	77.5	80.8	68.2
AttFuse [21]	89.3	82.6	87.5	76.0
CooPre	91.7 ^{+2.4}	86.6 ^{+4.0}	88.7 ^{+1.2}	80.0 ^{+4.0}

TABLE IV

RESULTS OF CROSS-DOMAIN TRANSFERABILITY OF OUR METHOD. RESULTS ARE DISPLAYED IN TERMS OF AP0.5 OF THE CAR CATEGORY.

GREEN DENOTES THE IMPROVEMENTS OVER THE TRAIN-FROM-SCRATCH BASELINE.

Pretrain	Finetune	V2V4Real	V2X-Real V2V
		No Pretrain	71.2
V2V4Real		74.3 ^{+3.1}	68.2 ^{+2.9}
V2X-Real V2V		72.2 ^{+1.0}	70.1 ^{+4.8}
Combined		74.5 ^{+3.3}	70.5 ^{+5.2}

synchronized and asynchronous modes. For OPV2V [21] dataset, we evaluate the performance of the vehicle class at the threshold of 0.5 and 0.7 at their two separate test sets.

Implementation Details. We evaluate our pretraining method using SECOND backbone [30]. Thus to have a fair comparison, we also train SECOND baseline method in V2X-Real [1] and V2V4Real [8]. All experiments are conducted in one Nvidia A6000 GPU. We employ AdamW [49] optimizer with a weight decay of 1×10^{-2} to optimize our models. During the pretraining stage, we train the model with a batch size of 4 for 15 epochs using a learning rate of 0.002, and we decay the learning rate with a cosine annealing [50]. We use a masking ratio of 0.7 in our main experiments and a fixed predicted point cloud number of 20. During the fine-tuning stage, the optimization process is identical to the train-from-scratch baselines. We finetune the model for 40 epochs in OPV2V dataset, 60 epochs in V2V4Real dataset, and 20 epochs in V2X-Real dataset. We also add normal point cloud data augmentations for all experiments, including scaling, rotation, and flip [28].

B. Main Results

In Table I, we present the experimental results across all collaboration modes in V2X-Real [1] dataset. In the VC and V2V settings, CooPre substantially outperforms the train-from-scratch baselines across all classification categories. The improvements are particularly notable in the Car and Truck categories, with a 4.4 mAP0.5 increase in the Car category and a 6.3 mAP0.5 increase in the Truck category in the VC setting, and a 4.8 mAP0.5 increase in the Car category and a 5.3 mAP0.5 increase in the Truck category in the V2V setting. This aligns with our pretraining design, which enables the model to learn more 3D geometrical and

TABLE V

EFFECTIVENESS OF COOPERATIVE AGENTS DURING PRETRAINING. RESULTS ARE DISPLAYED IN TERMS OF MAP0.5.

Dataset	Pretraining Mode	Overall	0-30m	30-50m	50-100m
V2X-Real VC	No Pretrain	48.5	61.0	53.5	36.9
	Ego pretraining	51.1	64.5	55.7	39.4
	V2X pretraining	52.2	64.9	55.9	42.1
V2X-Real V2V	No Pretrain	48.6	64.2	52.3	36.0
	Ego pretraining	50.5	65.4	54.6	38.7
	V2V pretraining	53.1	66.1	55.4	42.7

topological information beforehand, resulting in more accurate bounding box detection results with higher thresholds. On the other hand, the pretraining shows an incremental effect on detecting pedestrians. We attribute this to two factors: 1) pedestrians are small-scale in nature and thus receive fewer LiDAR features than larger objects, and 2) pedestrians are non-rigid-body objects, making it more challenging for the model to learn their 3D features compared to rigid-body counterparts such as cars and trucks. On the infrastructure side, our pretraining method shows improvements for the Car and Truck categories, but we observe a subtle decrease in the Pedestrian category. We attribute this to the small-scale and non-rigid-body nature of pedestrians, which might be negatively affected by asynchronous results transmitted from connected vehicles, such as pose and localization errors [13], [14]. This asynchronization can alter the perception accuracy of static infrastructure observers.

We show the generalizability of our method in another real-world dataset V2V4Real [8] and a simulation dataset OPV2V [21], as shown in Table II and Table III, respectively. For the V2V4Real dataset, after we pretrain and finetune the model, we test it under synchronized and asynchronous modes for a fair comparison. The improvement is substantial in both testing settings. For the OPV2V dataset, we outperform the baseline by a large margin across all test sets. These results demonstrate the generalizability of our pretraining method across different domains.

C. Data Efficiency

In this section, we investigate the benefits of our pretraining method in scenarios with limited labeled data. Specifically, we randomly sample 20%, 50%, and 80% of the training dataset and train the models with these annotated subsets. For our method, we pretrain the model on the entire training set and then finetune it on each sampled subset. As shown in Fig.5, our method outperforms train-from-scratch baselines across all settings. Notably, the performance gain of CooPre increases as the percentage of data decreases. Additionally, CooPre provides crucial guidance when collaboration involves different sensor configurations. For instance, in the V2X-Real VC dataset, the baseline method struggles to learn a good representation with limited annotations and the performance drops dramatically due to data heterogeneity issues. With our pretraining method, the model learns meaningful prior knowledge of different sensor distributions, leading to substantial improvements even when

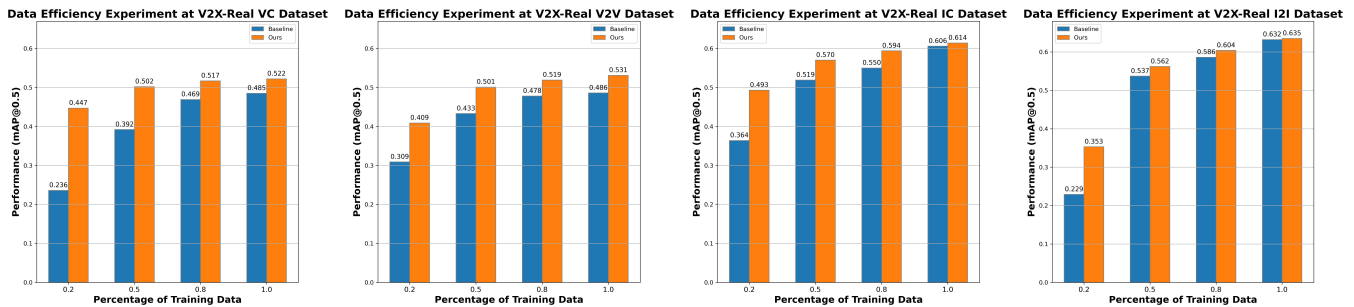


Fig. 5. **Data efficiency experiment.** We evaluate the performance boost using CooPre under different ratios of finetuning data on V2X-Real dataset.

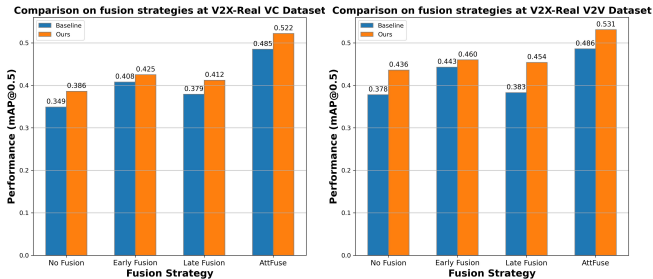


Fig. 6. **Comparison of CooPre across different cooperative fusion strategies.** We assess the performance enhancement provided by CooPre under various fusion strategies on the V2X-Real VC and V2V datasets.

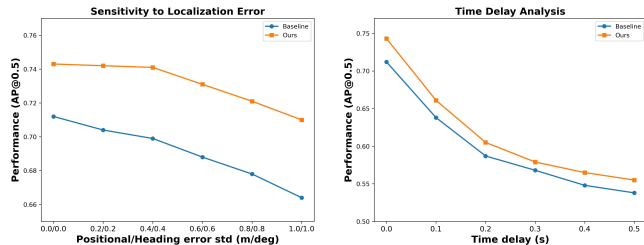


Fig. 7. **Robustness assessment on localization errors and time delay.** Our method shows strong robustness against localization errors and time delay compared to the train-from-scratch baseline on V2V4Real dataset.

finetuning with less labeled data. These findings demonstrate the effectiveness of our method in data scarcity scenarios.

D. Cross-domain Transferability

We evaluate the cross-dataset transferability of our pre-trained 3D encoder by finetuning it on another dataset. To isolate the effects of data heterogeneity, we investigate the performance across two real-world V2V datasets (V2X-Real V2V and V2V4Real), which have similar sensor configurations. As shown in Table IV, pretraining on a different domain improves performance compared to the train-from-scratch baseline. However, it performs worse than pretraining on the source domain due to the domain gap issue. We also conduct an experiment where we combine the V2X-Real V2V and V2V4Real datasets to create a large pretraining corpus. While this approach improves performance over pretraining on the source domain, the gains are less significant. This difference could be attributed to the scenario differences between the V2X-Real V2V and V2V4Real datasets. The

former primarily focuses on intersection scenarios, whereas the latter includes a broader range of corridor scenarios in its training set.

E. Ablation Studies

In this section, we conduct extensive experiments to explain how, where, and why our pretraining framework benefits current cooperative perception backbones.

Effectiveness of cooperative agents during pretraining.

To assess the impact of collaboration during pretraining, we compare the performance of our multi-agent pretraining method with the ego-agent pretraining method [18]. As shown in Table V, multi-agent cooperative pretraining leads to further improvements in model performance.

Extent of improvements in different perception ranges.

We also explore the enhancements across various perception ranges. As shown in Table V and Table II, the most substantial improvements are observed in middle and long ranges compared to the baselines. Given that our multi-agent pretraining method achieves a significantly larger perception field compared to the ego-agent pretraining method, our approach exhibits greater robustness in handling long-range perception and occlusions, as illustrated in Fig. 4.

Improvements with different cooperative fusion strategies. While our primary focus is on the intermediate fusion strategy, our method also applies to other fusion strategies, as depicted in Fig. 6. We observe that our pretraining strategy benefits other cooperative fusion strategies as well, with the intermediate fusion strategy consistently demonstrating the best performance.

Robustness assessment. Following [2], we evaluate our method’s robustness towards localization error and time delay compared to the baseline method on the V2V4Real dataset, as illustrated in Fig. 7. Our method is less sensitive to localization errors and shows its strong robustness against time delay.

Masking Ratio. Table VI demonstrates the effect of the masking ratio within the range of 0.6 to 0.8. With a masking ratio of 0.7, the pretraining framework achieves the best performance.

V. CONCLUSION

We introduce a multi-agent pretraining framework that prompts the representation to learn a holistic prior knowledge

TABLE VI
ABLATION ON MASKING RATIO.

Dataset	Mask Ratio	mAP0.3	mAP0.5
V2X-Real VC	0.6/0.7/0.8	59.1/ 60.1 /59.0	51.7/ 52.2 /51.0
V2X-Real V2V	0.6/0.7/0.8	57.6/ 59.5 /58.0	51.4/ 53.1 /51.6

of the 3D environment before performing the perception task. The framework explores the intrinsic geometrical and topological information of scenarios and sensor distributions. Extensive experiments on representative datasets demonstrate the efficacy of the method as it outperforms the previous state-of-the-art methods in all V2X settings. Furthermore, we demonstrate this framework’s strong generalizability, cross-domain adaptability, and data efficiency in cooperative perception. Future work includes extending this self-supervised cooperative pretraining paradigm to the field of cooperative perception and prediction task.

REFERENCES

- [1] H. Xiang, Z. Zheng, X. Xia, R. Xu, L. Gao, Z. Zhou, X. Han, X. Ji, M. Li, Z. Meng, *et al.*, “V2x-real: a largs-scale dataset for vehicle-to-everything cooperative perception,” *arXiv preprint arXiv:2403.16034*, 2024.
- [2] R. Xu, H. Xiang, Z. Tu, X. Xia, M.-H. Yang, and J. Ma, “V2X-ViT: Vehicle-to-Everything Cooperative Perception with Vision Transformer,” in *ECCV 2022*, ser. Lecture Notes in Computer Science, S. Avidan, G. Brostow, M. Cissé, G. M. Farinella, and T. Hassner, Eds. Cham: Springer Nature Switzerland, 2022, pp. 107–124.
- [3] Y. Li, D. Ma, Z. An, Z. Wang, Y. Zhong, S. Chen, and C. Feng, “V2X-Sim: Multi-Agent Collaborative Perception Dataset and Benchmark for Autonomous Driving,” *IEEE Robotics and Automation Letters*, vol. 7, no. 4, pp. 10914–10921, Oct. 2022, conference Name: IEEE Robotics and Automation Letters.
- [4] H. Yu, W. Yang, H. Ruan, Z. Yang, Y. Tang, X. Gao, X. Hao, Y. Shi, Y. Pan, N. Sun, J. Song, J. Yuan, P. Luo, and Z. Nie, “V2X-Seq: A Large-Scale Sequential Dataset for Vehicle-Infrastructure Cooperative Perception and Forecasting.” *arXiv*, May 2023, arXiv:2305.05938 [cs].
- [5] R. Hao, S. Fan, Y. Dai, Z. Zhang, C. Li, Y. Wang, H. Yu, W. Yang, Y. Jirui, and Z. Nie, “Rcooper: A real-world large-scale dataset for roadside cooperative perception,” in *Proceedings of the IEEE/CVF Conference on Computer Vision and Pattern Recognition (CVPR)*, 2024.
- [6] W. Zimmer, G. A. Wardana, S. Sritharan, X. Zhou, R. Song, and A. C. Knoll, “Tumtraf v2x cooperative perception dataset,” in *2024 IEEE/CVF International Conference on Computer Vision and Pattern Recognition (CVPR)*. IEEE/CVF, 2024.
- [7] Y. Li, Z. Li, N. Chen, M. Gong, Z. Lyu, Z. Wang, P. Jiang, and C. Feng, “Multiagent multitaversal multimodal self-driving: Open mars dataset,” in *Proceedings of the IEEE/CVF Conference on Computer Vision and Pattern Recognition (CVPR)*, June 2024, pp. 22 041–22 051.
- [8] R. Xu, X. Xia, J. Li, H. Li, S. Zhang, Z. Tu, Z. Meng, H. Xiang, X. Dong, R. Song, H. Yu, B. Zhou, and J. Ma, “V2V4Real: A Real-World Large-Scale Dataset for Vehicle-to-Vehicle Cooperative Perception,” 2023, pp. 13 712–13 722.
- [9] H. Caesar, V. Bankiti, A. H. Lang, S. Vora, V. E. Liong, Q. Xu, A. Krishnan, Y. Pan, G. Baldan, and O. Beijbom, “nusScenes: A multimodal dataset for autonomous driving,” in *Proceedings of the IEEE/CVF conference on computer vision and pattern recognition*, 2020, pp. 11 621–11 631.
- [10] M.-F. Chang, J. Lambert, P. Sangkloy, J. Singh, S. Bak, A. Hartnett, D. Wang, P. Carr, S. Lucey, D. Ramanan, and J. Hays, “Argoverse: 3D Tracking and Forecasting With Rich Maps,” 2019, pp. 8748–8757.
- [11] A. Geiger, P. Lenz, and R. Urtasun, “Are we ready for autonomous driving? the kitti vision benchmark suite,” in *2012 IEEE Conference on Computer Vision and Pattern Recognition*, 2012, pp. 3354–3361.
- [12] P. Sun, H. Kretzschmar, X. Dotiwalla, A. Chouard, V. Patnaik, P. Tsui, J. Guo, Y. Zhou, Y. Chai, B. Caine, V. Vasudevan, W. Han, J. Ngiam, H. Zhao, A. Timofeev, S. Ettinger, M. Krivokon, A. Gao, A. Joshi, Y. Zhang, J. Shlens, Z. Chen, and D. Anguelov, “Scalability in Perception for Autonomous Driving: Waymo Open Dataset,” 2020, pp. 2446–2454.
- [13] Y. Lu, Q. Li, B. Liu, M. Dianati, C. Feng, S. Chen, and Y. Wang, “Robust collaborative 3d object detection in presence of pose errors,” in *2023 IEEE International Conference on Robotics and Automation (ICRA)*. IEEE, 2023, pp. 4812–4818.
- [14] S. Wei, Y. Wei, Y. Hu, Y. Lu, Y. Zhong, S. Chen, and Y. Zhang, “Asynchrony-robust collaborative perception via bird’s eye view flow,” in *Advances in Neural Information Processing Systems*, 2023.
- [15] H. Xiang, R. Xu, X. Xia, Z. Zheng, B. Zhou, and J. Ma, “V2xp-arg: Generating adversarial scenes for vehicle-to-everything perception,” in *2023 IEEE International Conference on Robotics and Automation (ICRA)*, 2023, pp. 3584–3591.
- [16] Z. Zheng, X. Xia, L. Gao, H. Xiang, and J. Ma, “Cooperfuse: A real-time cooperative perception fusion framework,” in *2024 IEEE Intelligent Vehicles Symposium (IV)*, 2024, pp. 533–538.
- [17] Y. Li, S. Ren, P. Wu, S. Chen, C. Feng, and W. Zhang, “Learning distilled collaboration graph for multi-agent perception,” in *Thirty-fifth Conference on Neural Information Processing Systems (NeurIPS 2021)*, 2021.
- [18] Z. Lin, Y. Wang, S. Qi, N. Dong, and M.-H. Yang, “Bev-mae: Bird’s eye view masked autoencoders for point cloud pre-training in autonomous driving scenarios,” in *Proceedings of the AAAI conference on artificial intelligence*, 2024.
- [19] H. Yang, T. He, J. Liu, H. Chen, B. Wu, B. Lin, X. He, and W. Ouyang, “Gd-mae: Generative decoder for mae pre-training on lidar point clouds,” in *CVPR*, 2023.
- [20] X. Tian, H. Ran, Y. Wang, and H. Zhao, “Geomae: Masked geometric target prediction for self-supervised point cloud pre-training,” in *Proceedings of the IEEE/CVF Conference on Computer Vision and Pattern Recognition*, 2023, pp. 13 570–13 580.
- [21] R. Xu, H. Xiang, X. Xia, X. Han, J. Li, and J. Ma, “OPV2V: An Open Benchmark Dataset and Fusion Pipeline for Perception with Vehicle-to-Vehicle Communication,” in *2022 International Conference on Robotics and Automation (ICRA)*, May 2022, pp. 2583–2589.
- [22] T.-H. Wang, S. Manivasagam, M. Liang, B. Yang, W. Zeng, J. Tu, and R. Urtasun, “V2VNet: Vehicle-to-Vehicle Communication for Joint Perception and Prediction,” in *arXiv:2008.07519 [cs]*, Aug. 2020, 00010 ECC arXiv: 2008.07519.
- [23] Y. Hu, S. Fang, Z. Lei, Y. Zhong, and S. Chen, “Where2comm: Communication-efficient collaborative perception via spatial confidence maps,” *Advances in neural information processing systems*, vol. 35, pp. 4874–4886, 2022.
- [24] H. Yu, Y. Luo, M. Shu, Y. Huo, Z. Yang, Y. Shi, Z. Guo, H. Li, X. Hu, J. Yuan, and Z. Nie, “DAIR-V2X: A Large-Scale Dataset for Vehicle-Infrastructure Cooperative 3D Object Detection,” 2022, pp. 21 361–21 370.
- [25] R. Xu, Z. Tu, H. Xiang, W. Shao, B. Zhou, and J. Ma, “CoBEVT: Cooperative Bird’s Eye View Semantic Segmentation with Sparse Transformers.” *arXiv*, Sept. 2022, arXiv:2207.02202 [cs].
- [26] Q. Chen, X. Ma, S. Tang, J. Guo, Q. Yang, and S. Fu, “F-cooper: Feature based cooperative perception for autonomous vehicle edge computing system using 3d point clouds,” in *Proceedings of the 4th ACM/IEEE Symposium on Edge Computing*, 2019, pp. 88–100.
- [27] Z. Wu, Y. Wang, H. Ma, Z. Li, H. Qiu, and J. Li, “Cmp: Cooperative motion prediction with multi-agent communication,” *arXiv preprint arXiv:2403.17916*, 2024.
- [28] A. H. Lang, S. Vora, H. Caesar, L. Zhou, J. Yang, and O. Beijbom, “Pointpillars: Fast encoders for object detection from point clouds,” in *Proceedings of the IEEE/CVF conference on computer vision and pattern recognition*, 2019, pp. 12 697–12 705.
- [29] Y. Zhou and O. Tuzel, “VoxelNet: End-to-End Learning for Point Cloud Based 3D Object Detection,” 2018, pp. 4490–4499.
- [30] Y. Yan, Y. Mao, and B. Li, “Second: Sparsely embedded convolutional detection,” *Sensors*, vol. 18, no. 10, 2018. [Online]. Available: <https://www.mdpi.com/1424-8220/18/10/3337>
- [31] H. Xiang, R. Xu, and J. Ma, “HM-ViT: Hetero-modal Vehicle-to-Vehicle Cooperative perception with vision transformer,” Apr. 2023, arXiv:2304.10628 [cs].
- [32] Y. Lu, Y. Hu, Y. Zhong, D. Wang, S. Chen, and Y. Wang, “An extensible framework for open heterogeneous collaborative perception,”

in *The Twelfth International Conference on Learning Representations*, 2024.

- [33] J. Cheng, X. Mei, and M. Liu, "Forecast-MAE: Self-supervised pre-training for motion forecasting with masked autoencoders," *Proceedings of the IEEE/CVF International Conference on Computer Vision*, 2023.
- [34] H. Chen, J. Wang, K. Shao, F. Liu, J. Hao, C. Guan, G. Chen, and P.-A. Heng, "Traj-mae: Masked autoencoders for trajectory prediction," *2023 IEEE/CVF International Conference on Computer Vision (ICCV)*, pp. 8317–8328, 2023. [Online]. Available: <https://api.semanticscholar.org/CorpusID:257496187>
- [35] Y. Li, S. Z. Zhao, C. Xu, C. Tang, C. Li, M. Ding, M. Tomizuka, and W. Zhan, "Pre-training on synthetic driving data for trajectory prediction," 2023.
- [36] C. Xu, T. Li, C. Tang, L. Sun, K. Keutzer, M. Tomizuka, A. Fathi, and W. Zhan, "Pretram: Self-supervised pre-training via connecting trajectory and map," *arXiv preprint arXiv:2204.10435*, 2022.
- [37] C. Min, L. Xiao, D. Zhao, Y. Nie, and B. Dai, "Occupancy-mae: Self-supervised pre-training large-scale lidar point clouds with masked occupancy autoencoders," *IEEE Transactions on Intelligent Vehicles*, 2023.
- [38] Q. Li, Z. Peng, L. Feng, Q. Zhang, Z. Xue, and B. Zhou, "Metadrive: Composing diverse driving scenarios for generalizable reinforcement learning," *IEEE Transactions on Pattern Analysis and Machine Intelligence*, 2022.
- [39] Q. Li, Z. Peng, L. Feng, Z. Liu, C. Duan, W. Mo, and B. Zhou, "Scenarionet: Open-source platform for large-scale traffic scenario simulation and modeling," *Advances in Neural Information Processing Systems*, 2023.
- [40] K. He, X. Chen, S. Xie, Y. Li, P. Doll'ar, and R. B. Girshick, "Masked autoencoders are scalable vision learners," *2022 IEEE/CVF Conference on Computer Vision and Pattern Recognition (CVPR)*, pp. 15 979–15 988, 2021. [Online]. Available: <https://api.semanticscholar.org/CorpusID:243985980>
- [41] C. Feichtenhofer, H. Fan, Y. Li, and K. He, "Masked autoencoders as spatiotemporal learners," *ArXiv*, vol. abs/2205.09113, 2022. [Online]. Available: <https://api.semanticscholar.org/CorpusID:248863181>
- [42] P. Gao, T. Ma, H. Li, J. Dai, and Y. Qiao, "Convmae: Masked convolution meets masked autoencoders," *arXiv preprint arXiv:2205.03892*, 2022.
- [43] R. Zhang, Z. Guo, P. Gao, R. Fang, B. Zhao, D. Wang, Y. Qiao, and H. Li, "Point-m2ae: Multi-scale masked autoencoders for hierarchical point cloud pre-training," *arXiv preprint arXiv:2205.14401*, 2022.
- [44] X. Yu, L. Tang, Y. Rao, T. Huang, J. Zhou, and J. Lu, "Point-bert: Pre-training 3d point cloud transformers with masked point modeling," in *Proceedings of the IEEE Conference on Computer Vision and Pattern Recognition (CVPR)*, 2022.
- [45] Y. Pang, W. Wang, F. E. Tay, W. Liu, Y. Tian, and L. Yuan, "Masked autoencoders for point cloud self-supervised learning," in *Computer Vision—ECCV 2022: 17th European Conference, Tel Aviv, Israel, October 23–27, 2022, Proceedings, Part II*. Springer, 2022, pp. 604–621.
- [46] D. Huang, S. Peng, T. He, H. Yang, X. Zhou, and W. Ouyang, "Ponder: Point cloud pre-training via neural rendering," in *Proceedings of the IEEE/CVF International Conference on Computer Vision*, 2023, pp. 16 089–16 098.
- [47] H. Zhu, H. Yang, X. Wu, D. Huang, S. Zhang, X. He, T. He, H. Zhao, C. Shen, Y. Qiao, and W. Ouyang, "Ponderv2: Pave the way for 3d foundation model with a universal pre-training paradigm," *arXiv preprint arXiv:2310.08586*, 2023.
- [48] B. Wang, L. Zhang, Z. Wang, Y. Zhao, and T. Zhou, "Core: Cooperative reconstruction for multi-agent perception," *2023 IEEE/CVF International Conference on Computer Vision (ICCV)*, pp. 8676–8686, 2023. [Online]. Available: <https://api.semanticscholar.org/CorpusID:260091736>
- [49] D. P. Kingma and J. Ba, "Adam: A method for stochastic optimization," *arXiv preprint arXiv:1412.6980*, 2014.
- [50] I. Loshchilov and F. Hutter, "Decoupled weight decay regularization," in *International Conference on Learning Representations*, 2019. [Online]. Available: <https://openreview.net/forum?id=Bkg6RiCqY7>